Turun yliopisto
University of Turku

ON THE EFFECT OF MOLECULAR STRUCTURE AND COMPOSITION ON THE PHOTOFRAGMENTATION OF BIOMOLECULES

Helena Levola

TURUN YLIOPISTON JULKAISUJA – ANNALES UNIVERSITATIS TURKUENSIS
Sarja - ser. AI osa - tom. 538 | Astronomica - Chemica - Physica - Mathematica | Turku 2016

University of Turku

Faculty of Mathematics and Natural Sciences
Department of Physics and Astronomy
Materials research laboratory

Supervised by

Professor Edwin Kukk
Department of Physics and Astronomy
University of Turku
Turku, Finland

Ph.D. Kuno Kooser
Department of Physics and Astronomy
University of Turku
Turku, Finland

Reviewed by

Assoc. Professor Dr. Stephan Denifl
Institut für Ionenphysik und Angewandte Physik
Innsbruck, Austria

Professor Dr. Matjaž Žitnik
Jožef Stefan Institute
Department of low and medium energy physics
Ljubljana, Slovenia

Opponent

Ph.D. Kevin C. Prince
Elettra-Sincrotrone Trieste
Basovizza, Italy

ISBN 978-951-29-6459-8 (PRINT)
ISBN 978-951-29-6460-4 (PDF)
ISSN 0082-7002 (Print)
ISSN 2343-3175 (Online)
Painosalama Oy - Turku, Finland 2016

"The aim of science is not to find absolute truths
but to find the least wrong answers"
– Robin Ince

Acknowledgements

These words that appear at the end of my long journey as a doctoral candidate are hardly enough to describe the deep gratitude I feel. I can only try and express my gratefulness to so many people.

No one deserves my thanks more than my wonderful supervisors, Prof. Edwin Kukk and Dr. Kuno Kooser. Edwin has not only been an excellent thesis supervisor, but he has also offered me plenty of opportunities to experience and explore science beyond my own research. My other supervisor, Kuno, has shown me the practical side of experimental work and in so doing he has been extremely patient. Being a spoilt white collar worker, I was completely lost among all the equipment and machines necessary to an experimental physicist. Fortunately, Kuno never gave up on me but insisted that I tried and learned.

My colleagues in materials research laboratory have also played an important role in my development as a scientist. I want to thank Docent Jarkko Leiro for sharing his vast repertoire of historical stories that were both educating and entertaining. I would also like to thank our former laboratory engineer Markku Heinonen for helping me with laboratory related problems, although it was strictly not his responsibility. I thank Dr. Taina Laiho for the fruitful discussions about academic life and Dr. Sari Granroth for helping me with school group visits. Both Sari and Taina deserve special thanks for always putting an effort to organize some team-building activities outside work. The former graduate students of our laboratory, Doctors Dang Trinh Ha and Eero Itälä, also have my gratitude. I am very grateful to Dani for always finding the time to help me with quantum mechanical problems. I am indebted to Eero for passing on his knowledge, both practical and theoretical, about the research done by our group before I joined it. I also thank our present graduate students, Tiina Kilpi and Marta Tarkanovskaja, for their many questions that forced me to think and learn so much myself.

In addition to our people in materials science, I would like to thank my colleague graduate student from the materials physics laboratory, Marjukka Tuominen. It has been a pleasure to grow up as scientists together and share experiences from both sides of materials research.

During my years as a graduate student I have also received an enormous support from my family. I thank my father for the “genes for physics” and for the financial support he has given for my studies. I thank my brother for always encouraging me to learn more, to know more and to educate myself, also outside my own field of interest. I thank my mother for the help in eve-

ryday matters so that my work would go smoother. I especially thank her for taking care of the cat while I was away on work assignments. Knowing that he was on good hands let me concentrate fully on my work.

Finally, I want to express my gratitude towards my spouse, Jere, who has been there for me all these years. He has shared all the joys and the sorrows with me, and most importantly, he has always believed in me. Life would have been much harder without him beside me.

Abstract

The research on the interaction between radiation and biomolecules provides valuable information for both radiobiology and molecular physics. While radiobiology is interested in the damage inflicted on the molecule upon irradiation, molecular physics exploits these studies to obtain information about the physical properties of the molecule and the quantum mechanical processes involved in the interaction.

This thesis work investigated how a small change in the structure or composition of a biomolecule changes the response of the molecule to ionizing radiation. Altogether eight different biomolecules were studied: nucleosides uridine, 5-methyluridine and thymidine; amino acids alanine, cysteine and serine; and halogenated acetic acids chloro- and bromoacetic acids. The effect of ionizing radiation on these molecules was studied on molecular level, investigating the samples in gas phase. Synchrotron radiation of VUV or soft x-ray range was used to ionize sample molecules, and the subsequent fragmentation processes were investigated with ion mass spectroscopy and ion-ion-electron coincidence spectroscopy.

The comparison between the three nucleosides revealed that adding or removing a single functional group can affect not only the bonds from which the molecule ruptures upon ionization but also the charge localization in the formed fragments. Studies on amino acids and halogenated acetic acids indicated that one simple substitution in the molecule can dramatically change the extent of fragmentation. This thesis work also demonstrates that in order to steer the radiation-induced fragmentation of the molecules, it is not always necessary to alter the amount of energy deposited on the molecules but selecting a suitable substitution may suffice.

Tiivistelmä

Biomolekyylien ja säteilyn välisten vuorovaikutusprosessien tutkiminen on olennaista sekä säteilybiologialle että molekyylifysiikalle. Säteilybiologia tarkastelee säteilyn molekyyliin aiheuttamia vaurioita, kun taas molekyylifysiikka hyödyntää näitä tutkimuksia saadakseen tietoa molekyylin fysikaalisista perusominaisuuksista ja vuorovaikutusprosessien kvanttimekaanisista tapahtumaketjuista.

Tässä väitöskirjatyössä tutkittiin, miten pieni muutos biomolekyylin rakenteessa tai koostumuksessa muuttaa molekyylin tapaa reagoida ionisoivaan säteilyyn. Tutkimuskohteiksi valittiin kahdeksan erilaista biomolekyyliä: nukleosidit uridiini, 5-metyyliuridiini ja tymidiini; aminohapot alaniini, kysteiini ja seriini; ja kaksi halogenoitua etikkahappoa, kloori- ja bromietikkahapot. Ionisoivan säteilyn vaikutusta näihin molekyyleihin tarkasteltiin molekyylitasolla tutkimalla näytemolekyylejä kaasufaasissa. Näytemolekyylit ionisoitiin VUV:n tai pehmeän röntgensäteilyn alueen synkrotronisäteilyllä, ja ionisaation jälkeistä molekyylin hajoamista tutkittiin ionien massaspektroskopialla ja ioni–ioni–elektroni-koinsidenssispektroskopialla.

Kolmen nukleosidin vertailu paljasti, että yhden funktionaalisen ryhmän lisääminen tai poistaminen voi vaikuttaa paitsi siihen, mitkä sidokset molekyylissä katkeavat, myös siihen mihin muodostuneista hajoamistuotteista ionisaation tuottama sähköinen varaus jää. Aminohappojen ja halogenoitujen etikkahappojen tutkimukset puolestaan osoittivat, että pelkkä substituution vaihtaminen voi merkittävästi muuttaa molekyylin hajoamisen astetta. Tämä väitöskirjatutkimus myös osoittaa, että säteilyn aiheuttamaa molekyylin hajoamista voidaan hallita paitsi muuttamalla molekyylin kohdistuvan energian määrää, myös valitsemalla sopiva substituutio.

Contents

List of Papers

This thesis includes the following research papers.

I. H. Levola, K. Kooser, E. Rachlew, E. Nõmmiste, and E. Kukk: *Fragmentation of thymidine induced by ultraviolet photoionization and thermal degradation,* International Journal of Mass Spectrometry 353 (2013), 7.

II. H. Levola, K. Kooser, E. Itälä, and E. Kukk: *Comparison of VUV induced fragmentation of thymidine and uridine nucleosides – The effect of methyl and hydroxyl groups*, International Journal of Mass Spectrometry 370 (2014), 96.

III. E. Itälä, K. Kooser, E. Rachlew, H. Levola, D.-T. Ha, and E. Kukk: *Photofragmentation of uridine following C 1s core ionization,* The Journal of Chemical Physics 142 (2015), 194303.

IV. H. Levola, E. Itälä, K. Schlesier, K. Kooser, S. Laine, J. Laksman, D. T. Ha, E. Rachlew, M. Tarkanovskaja, K. Tanzer, and E. Kukk: *Ionization-site effects on the photofragmentation of chloro-and bromoacetic acid molecules*, Physical Review A 92 (2015), 063409.

V. J. Laksman, K. Kooser, H. Levola, E. Itälä, D. T. Ha, E. Rachlew, and E. Kukk: *Dissociation pathways in the cysteine dication after site-selective core ionization*, The Journal of Physical Chemistry, Part B, 118 (2014), 11688.

VI. E. Itälä, H. Levola, D. T. Ha, K. Kooser, E. Rachlew, and E. Kukk: *Photofragmentation of serine following C 1s ionization - comparison with cysteine*, manuscript submitted to The Journal of Physical Chemistry, Part B in March 2016.

The author's contribution to the papers has been the following. In all papers, she participated in the experimental measurements. In papers I, II and IV, she also analyzed the measured data and was responsible for writing the articles.

In addition to the papers listed above, the author has been involved in the following publications not included in the thesis work:

E. Kukk, D. T. Ha, Y. Wang, D. G. Piekarski, S. Diaz-Tendero, K. Kooser, E. Itälä, H. Levola, M. Alcamí, E. Rachlew, and F. Martín: *Internal energy dependency in X-ray induced molecular fragmentation – an experimental and theoretical study on thiophene,* Physical Review A 91 (2015), 043417.

J. Laksman, E. Itälä, D. T. Ha, K. Kooser, K. Schlesier, H. Levola, E. Rachlew, and E. Kukk: *Experimental evidence for conformer dependence on the dissociation dynamics of thiazole-2-carboxylic acid cation*, manuscript submitted to Physical Chemistry Chemical Physics.

1 INTRODUCTION

The interaction between ionizing radiation and biomolecules has been a popular study subject for decades. Its obvious importance to radiobiology and medicine has been one of the main motivations. Other interests come from industrial applications that use biomaterials exposed to radiation, e.g. paints, plastics or organic electronic devices. In molecular physics' point of view, investigating ionization processes provides information about physical properties of the molecule and quantum mechanical processes involved.

In addition to being biologically relevant, biomolecules are a fruitful study subject in molecular physics due to their structural variety. Biomolecules often have several different forms, existing in different geometrical and spatial arrangements or conformers. Many of them differ from some other molecule only by a single functional group. Moreover, they can be easily modified by substituting one atom by another element or a functional group. For instance, hydrogen can be substituted by a heavier atom such as bromine or chlorine, or by a methyl group. This diversity of biomolecules enables one to study how a small change in a molecular structure or composition affects the behavior of a molecule. The information gathered in such comparative studies is valuable in the quest of developing a quantum mechanical description of matter.

Experimentally, radiation damage to biomolecules can be studied by various spectroscopic methods including x-ray absorption [1] and emission [2] spectroscopies, ion mass spectroscopy [3], and electron spectroscopy [4]. Ionization often leads to breakages of one or more molecular bonds and eventually to fragmentation of the molecule. Mass spectra of the molecule reveal from which bonds the molecule tends to break. Kinetic energies of the emitted electrons, on the other hand, contain information about elec-

tronic energies involved in the fragmentation. Combining these two spectroscopies, detecting emitted ions and electrons simultaneously, allows one to create a more complete picture of the ionization process. This so-called coincidence spectroscopy [5] enables one to determine the sequence of the fragmentation process. Moreover, it can be used to study how the fragmentation depends on the ionization site or on the internal energy of the molecule.

Regarding radiation damage, the DNA molecule is considered to be the most crucial molecule in biological tissues. Being a rather large molecule it is an easy target and damage to it may be lethal to the cells [6]. The size of the DNA molecule also makes it a challenging study subject. Therefore, molecular physicists often adopt a so-called 'bottom-up' method, in which smaller parts of the bigger target molecule are studied first and when enough information is gathered, the size of the sample molecule can be increased. In case of the DNA, the smaller study subjects are usually individual nucleobases and deoxy-D-ribose sugars or their combinations, nucleosides. The bottom-up method can also be applied to other biologically important macromolecules. In case of proteins, for example, single amino acids can be used as a starting point in radiation damage studies.

In this thesis work, spectroscopic methods are employed in order to study radiation damage to smaller constituents of proteins and DNA and RNA molecules. Carboxylic acids and amino acids are taken as representatives of proteins and the nucleosides thymidine and uridine are chosen as samples of DNA and RNA, respectively. The structures of the molecules studied in this thesis work are depicted in Figure 1.

This thesis is organized in four chapters. The next chapter, chapter 2, introduces relevant concepts related to ionization and subsequent fragmentation processes of biomolecules. The third chapter describes the used experimental methods, and the final chapter summarizes and discusses the results of the research papers.

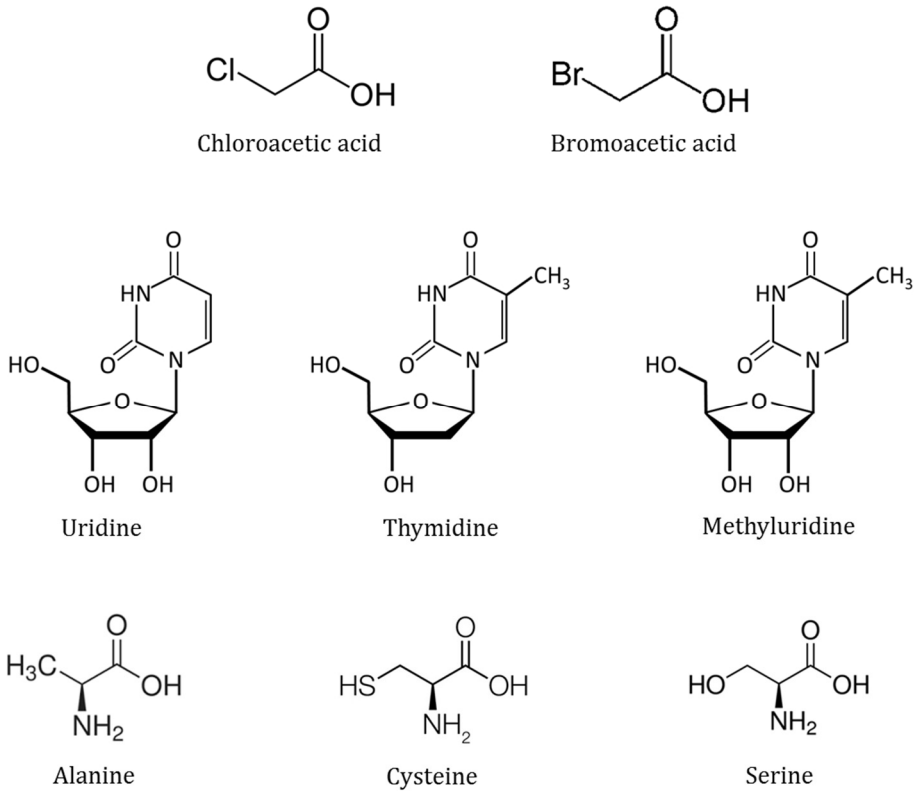

Figure 1. Sample molecules studied in this thesis work.

2 PHOTOFRAGMENTATION OF MOLECULES

Interaction between photons and atoms or molecules can occur in multiple ways, including scattering and absorption that can lead to excitation or ionization. Scattering processes can be categorized as elastic or inelastic depending on whether no energy or part of the energy is transferred from the photon to the system. When a photon with initial energy $h\nu_1$ scatters inelastically from a molecule M, it loses part of its energy and departs with a decreased energy $h\nu_2$. The energy difference $h\nu_1 - h\nu_2$ can be consumed either by excitation of the molecule,

$$h\nu_1 + M \rightarrow h\nu_2 + M^*, \tag{1}$$

or, with large enough energy differences, by ionization of the molecule,

$$h\nu_1 + M \rightarrow h\nu_2 + M^+ + e^-. \tag{2}$$

In contrast to scattering processes, absorption processes entail annihilation of the photon and transfer of all its energy to the system. As in scattering processes, the absorbed energy can be consumed either by excitation,

$$h\nu_1 + M \rightarrow M^*, \tag{3}$$

or ionization of the system,

$$h\nu_1 + M \rightarrow M^+ + e^-. \tag{4}$$

The probability of each interaction process is strongly affected by incident photon energy (see Figure 2). With the photon energies used in this thesis work, from 7 to 600 eV, ionization is the most relevant process to be considered. When a molecule is excited or ionized, the energy deposited on the molecule may be so large that it is capable of breaking the bonds be-

tween the constituent atoms leading to fragmentation of the molecule. When the molecule is ionized with photon radiation, the subsequent fragmentation is often called photofragmentation to differentiate it from ionization with electrons, for example, or from fragmentation processes unrelated to radiation. Similarly, electrons emitted in photoabsorption are called photoelectrons. In this chapter, physical aspects related to ionization and photofragmentation of molecules are discussed.

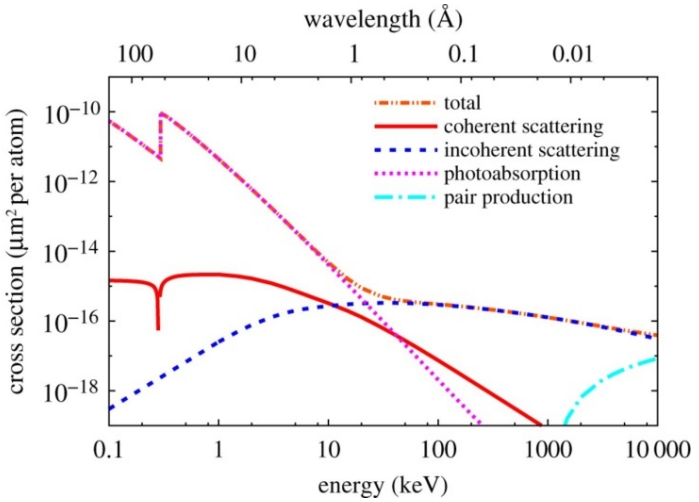

Figure 2. Dependence of cross-sections on the photon energy for the example of carbon atom [7].

2.1 Molecular orbitals

Before discussing ionization or fragmentation of molecules, it is beneficial to consider the structure of a molecule. A molecule is often described as an ensemble of atomic nuclei surrounded by circulating electrons. Being quantum mechanical particles, electrons are best described by probabilities of their position and energy rather than deterministic trajectories. The wavefunctions that determine the spatial distributions of electrons in a molecule are called *molecular orbitals* and they can be used to describe the electronic structure of a molecule. Knowing the exact electronic structure of the molecule would require solving the Schrödinger equation. The Coulombic repulsion potential between the electrons, however, makes an analytical solution impossible and various approximation methods have been developed.

One numerical method to solve the Schrödinger equation of a multielectron system is called Hartree–Fock self-consistent field (HF-SCF) method. It

was first introduced by Douglas Hartree in 1928 [8] and was further developed by John Slater [9-10] and Vladimir Fock [11]. The HF-SCF method does not only take the Coulombic repulsion into account but also the exchange interaction of the electrons. The starting point in this method is that an electron moves in an average electric field created by the other electrons and by fixed nuclei. In order to calculate the average electric field, assumptions about the wavefunctions of the other electrons have to be made. The average electric field based on these assumed wavefunctions is then used to solve Schrödinger equations of all electrons. After the first calculation round, a set of new wavefunctions has been acquired and it is inserted into Schrödinger equations to find a new, improved set of wavefunctions. This iterative process continues until the improved versions of the wavefunctions do not differ significantly from the versions in the beginning of the calculation round.

The question in the HF-SCF method now becomes how to select the first versions of the wavefunctions. A very common approach is to construct the initial wavefunctions ψ_m as linear combinations of atomic orbitals (LCAO),

$$\psi_m = \sum_{i=1}^{N} c_{im}\chi_i \,, \tag{5}$$

where c_{im} are constants related to a molecular orbital m and atom i, and χ_i are the atomic orbitals belonging to atom i in a molecule. Use of the LCAO method is appealing because it transforms the problem of optimizing wavefunctions into optimizing coefficients c_{im}, and because plenty of good atomic orbital approximations for multielectron atoms are available [12]. One option for the atomic orbitals or the basis functions χ_i is the Gaussian-type orbitals (GTOs) [13] that are defined by an equation

$$g_{ijk}(r) = Nx^i y^j x^k e^{-\alpha r^2} \tag{6}$$

where N is a normalization constant, i, j, and k are non-negative integers, and α is a positive constant. The integers i, j and k define the type of the atomic orbitals. If they are all zero, for example, the orbital is s-type, and if their sum $i+j+k$ equals one, the orbital is p-type. The GTOs can also be grouped together into so-called *contracted Gaussian functions* where linear combinations of g_{ijk} centered at the same atomic nucleus are used instead of primitive GTOs given by Eq. 6. Using contracted GTOs reduces the number of basis functions and facilitates the calculations [12].

The qualities of the wavefunctions can be used to divide molecular orbitals in three classes. *Core orbitals* are well localized around a nucleus and

they are low in energy. The main contribution to these orbitals comes from solitary atomic core orbitals. *Valence orbitals* have higher energies and they are spread over larger area in a molecule. *Unoccupied orbitals* are located above the valence orbitals, and as their name suggests, they usually do not contain electrons. They can, however, accept electrons from lower orbitals in excitation processes, or from surrounding atoms or molecules. The contraction schemes of GTOs typically involve different basis sets for inner shell and valence shell orbitals. For example, in the contraction scheme 6-31G used in paper IV of this thesis, one contracted Gaussian composed of six primitives is used for the inner shells while the valence shells are constructed with one contracted Gaussian composed of three primitives and a single diffuse primitive function.

As an example of the use of LCAO in construction of molecular orbitals, the molecular orbitals of chloroacetic acid molecule in neutral ground state are presented in Figure 3. These orbitals were obtained by HF-SCF calculations using 6-31G(d) basis set [14-17]. The calculations were performed with GAMESS quantum chemistry code [18] via WebMo interface [19]. The molecular orbitals in Figure 3 demonstrate well the different nature of core and valence orbitals. The orbitals 1-9 are clearly concentrated around specific atoms and have significantly lower energies than the other orbitals: they correspond to the core orbitals. The lowest orbital (MO1) is so contracted that its size is smaller than the chlorine atom in the picture; this orbital is essentially the atomic core orbital 1*s* of chlorine. The next lowest orbitals, MO2 and MO3, are located around the two oxygen atoms, and they correspond to the 1*s* orbitals of the oxygens. Above them in energy follow orbitals 4 and 5 that correspond to the 1*s* orbitals the carbon atoms, and orbitals 6-9 that have contributions from the 2*p* orbitals of chlorine. Compared with the core orbitals, the orbitals 10-24 are much higher in energy and they are spread more over the molecule. They constitute the valence orbitals, which are linear combinations of multiple atomic orbitals.

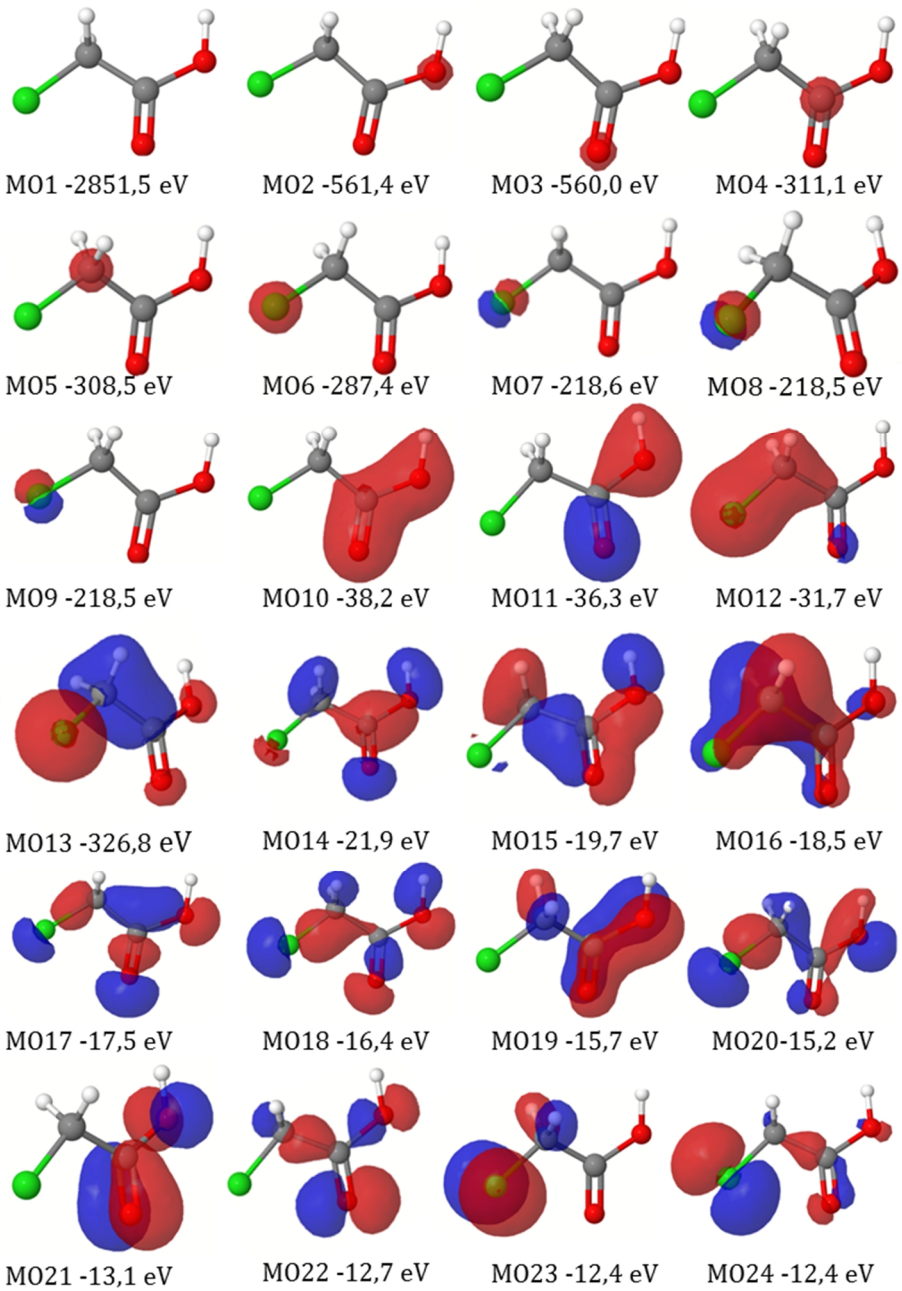

Figure 3. Molecular orbitals of chloroacetic acid molecule obtained by HF method (see text for more details on the calculations). The molecular orbitals 1-9 correspond to core orbitals and orbitals 10-24 to valence orbitals. The rotation of the molecule is slightly different in some orbital images to provide better view of the orbital structure.

2.2 Photoionization and photoelectron spectra

Although the mathematical description of the molecular orbitals remains more or less approximate, they are a useful concept in discussions of various molecular phenomena. Ionization, for instance, can be conceived as a process that leads to a removal of an electron from a molecular orbital to continuum. The minimum amount of energy required to detach an electron from an orbital and promote it to continuum is called *ionization energy* or *ionization threshold*. In quantum mechanical point of view, the probability that a photon ionizes an electron is determined by the transition moment μ:

$$\mu = \int \phi \times \boldsymbol{r} \times \varepsilon \; d^3\boldsymbol{r} \;, \tag{7}$$

where ϕ and ε denote the wavefunctions of bound and continuum electrons, respectively, and $\boldsymbol{r}$ represents the dipole operator. The qualitative interpretation of Eq. 7 is that ionizing an electron from a certain orbital requires that the wavefunctions of the bound electron (ϕ) and that of the continuum electron (ε) overlap. This overlap depends on the photon via the energy that it deposits on a bound electron, as illustrated in Figure 4. In broader terms, the interaction probability of radiation and matter is described with a parameter called cross-section which includes the effect of transition moment. Cross-section is highest for photon energies near the ionization threshold and decreases with increasing photon energy.

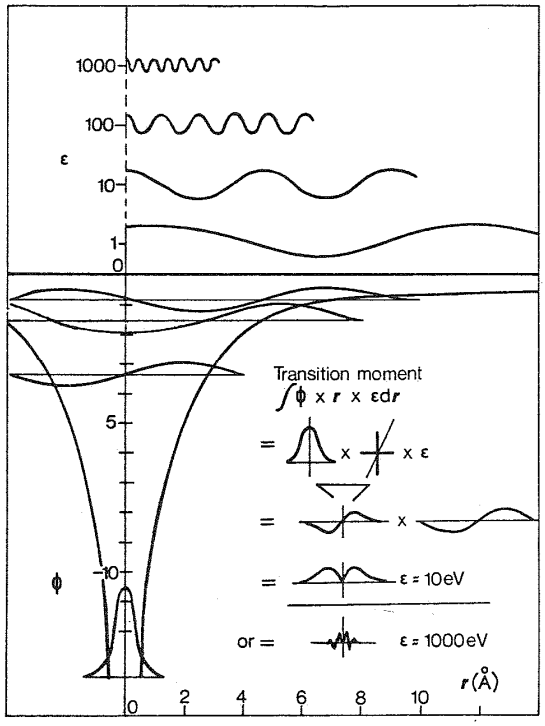

Figure 4. Illustration of the transition moment of an ionization process [20].

According to Koopmans' approximation, orbital energy ε_m equals the negative value of the electron's ionization energy E_{ion}:

$$E_{ion} = -\varepsilon_m \ . \tag{8}$$

Thus, the primary information provided by photoelectron spectra is the molecular orbital energies, which can offer plenty of secondary information about the molecule. For example, core-level photoelectron spectra can in some cases reveal information about the molecular structure. The core orbital energies of the elements change slightly when the atoms are bonded together to form molecules. This so-called *chemical shift* can be observed in photoelectron spectra as displacements of photoelectron peaks related to peak positions of free atoms. The shift depends on the neighboring atoms of the studied orbital. Therefore, by analyzing the chemical shifts it is sometimes possible to deduce the way the atoms are bonded together and to construct an image of the molecule in question. In paper III, for instance, chemical shifts were used to conclude that gas-phase uridine molecule exists in pyranose rather than furanose form. Chemical shifts can also be used to differentiate atoms of same element in electron-ion coincidence meas-

urements, which is helpful, for example, in site-selective fragmentation studies (see Section 2.3).

2.3 Site-selective vs. site-dependent fragmentation

Since atomic core orbitals preserve their localized nature even when the atoms are bonded together to form a molecule, core ionization creates a hole essentially at a distinct location in the molecule. With this *site-selective ionization* method it is possible to study how the location of the initial core hole affects the fragmentation behavior of the molecule. The problem with site-selective ionization is, however, that multiple ionization or excitation processes may be initiated with a given photon energy. Therefore, the observed fragmentation may not be exclusively related to ionization of a certain core level. In addition, site-selective ionization does not distinguish between atoms of same elements. These problems can be avoided if the fragmentation is observed in coincidence with the emitted photoelectrons. Observing fragmentation with certain core level photoelectrons filters out any other fragmentation processes that might occur with the same photon energy. Moreover, measuring the energies of photoelectrons provides a means to separate atoms of same elements based on their chemical shifts, provided that the electron energy resolution is less than the chemical shift.

In some molecules, the initial ionization site has been observed to have a significant impact on photofragmentation. The ionization site can in some cases determine from which bonds the molecule is cut; this is called *site-selective fragmentation*. More often, however, site-selective ionization leads to changes in probabilities or branching ratios of different fragmentation pathways rather than in the fragmentation pathways themselves. This behavior is called *site-dependent fragmentation.* Various mechanisms for site-selective or site-dependent fragmentation have been suggested and they are reviewed in length in the introduction section of paper IV. One of the proposed reasons for site-dependent effects is so-called internal energy and it is discussed in the next section.

2.4 Auger process and internal energy

After core ionization, the molecular ion is left in an excited state and it will relax to the ground state either by fluorescence or Auger emission, the latter process being more probable in light elements. In Auger emission, the core hole is filled by another electron from orbitals higher in energy than

the orbital containing the core hole. The released energy is consumed by emission of a second electron called *Auger electron.*

The core-ionized states of biomolecules usually decay by Auger emission and, therefore, core ionization leads to at least doubly charged biomolecules. The energy of these final dicationic states depends on which molecular orbitals are involved in the Auger process. The lowest final state energy is achieved when the Auger process creates two holes in the highest occupied molecular orbital (HOMO). If the core holes are created in lower molecular orbitals, the final state energy increases. The correlation between kinetic energy of an Auger electron and the final state energy of the molecule is illustrated in Figure 5.

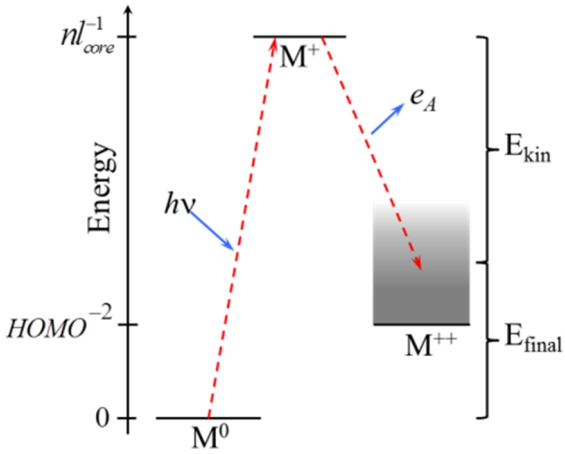

Figure 5. Correlation between final state energy of the molecule and kinetic energy of the Auger electron. Picture is taken from paper IV.

Since Auger electrons carry with them information about the final state energy, Auger electron spectroscopy is an excellent method to study it. If the kinetic energies of Auger electrons E_{Auger} are known, the final state energies E_{final} can be calculated from the equation:

$$E_{final} = E_{core} - E_{Auger} \ , \tag{9}$$

where E_{core} denotes the ionization energy of the core orbital. Occasionally, the difference between the dicationic ground state energy (marked M^{++} in Figure 5) and the final state energy is used rather than the absolute final state energy. This energy difference is called *internal energy*. In order to calculate the amount of internal energy, the double ionization energy has to be known. This information is not always available; however, since final

state energy is directly linked to internal energy, these terms are sometimes used interchangeably.

After Auger decay, the molecule is multiply charged and it will fragment in a Coulomb explosion. If the formed fragment ions are measured in coincidence with the emitted Auger electrons, it is possible to investigate the involvement of final state energy or internal energy on the fragmentation.

3 EXPERIMENTAL METHODS

In this thesis work, ion time-of-flight mass spectroscopy (ion TOF MS) and photoelectron-ion-ion-coincidence (PEPIPICO) spectroscopy were used to study fragmentation of various biomolecules. Synchrotron radiation in vacuum ultraviolet (VUV) or soft x-ray region was used to ionize the molecules. In auxiliary measurements carried out in the home laboratory of Materials Research of University of Turku, a gas discharge lamp was also used as radiation source. In the following sections, a more detailed description of each aspect of the experimental methods is given.

3.1 Synchrotron radiation

Synchrotron radiation is created when relativistic electrons follow a circular or oscillating path. The continuously changing direction of their velocities means that they have acceleration and this acceleration is manifested in the production of electromagnetic radiation. With relativistic energies, the radiation is emitted in a narrow cone directed along the tangent of the path of the electrons.

3.1.1 Structure of a synchrotron

The main parts of the type of synchrotron used in this thesis work are depicted in Figure 6. Electrons are accelerated to high velocities in a linear accelerator after which they may be further accelerated in a smaller ring structure called the booster ring. When the electrons have acquired a sufficient kinetic energy, typically a few GeV, they are released into a storage ring where they circulate emitting photon radiation. The radiation is guided

to the sample by beamlines that both transport the radiation and select a spectral slice suitable for the measurements. At the very end of a beamline, there is an experimental station that consists of spectroscopic equipment.

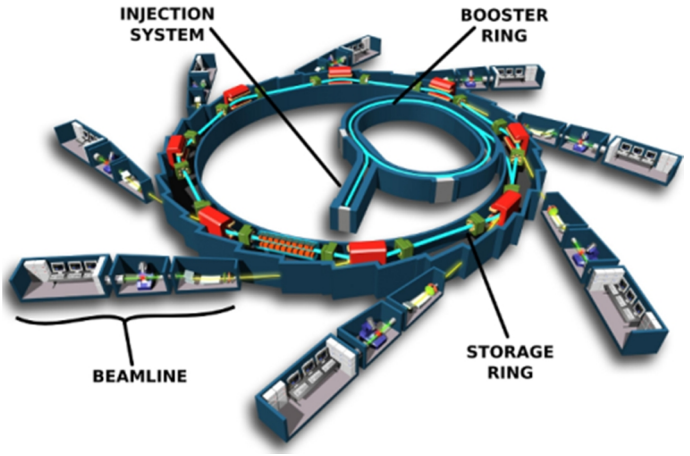

Figure 6. The main parts of a synchrotron: injection system, booster ring, storage ring and beamlines [21].

The path of the electrons is primarily guided by bending magnets, but the storage ring also contains straight sections in which different kinds of devices can be installed to further modify the path of the electrons and the properties of the emitted electromagnetic radiation. The most important one of these so-called insertion devices is a magnetic structure called an undulator. In this thesis work, all the measurements using synchrotron radiation were carried out at undulator beamlines and, therefore, the emphasis of this section is on the description of undulator radiation.

3.1.2 Properties of undulator radiation

Undulators are magnetic structures that consist of two arrays of magnets separated by a gap. The magnets are arranged in such a way that the poles alternate (see Figure 7). When an electron enters the undulator, magnetic forces cause its path to oscillate in a plane perpendicular to the magnetic field. The oscillation period λ_u is determined by the distance between two magnets of same polarity and is also called the undulator spatial period. The magnetic field strength is relatively weak, and the oscillations occur within the produced radiation cone. The interference of the emitted photons will lead to constructive interference of only certain wavelengths and as a result, the undulator radiation spectrum is not continuous but discrete (see Figure

8). In addition, being confined in a small cone, the emitted radiation is significantly brighter than achieved with bending magnets.

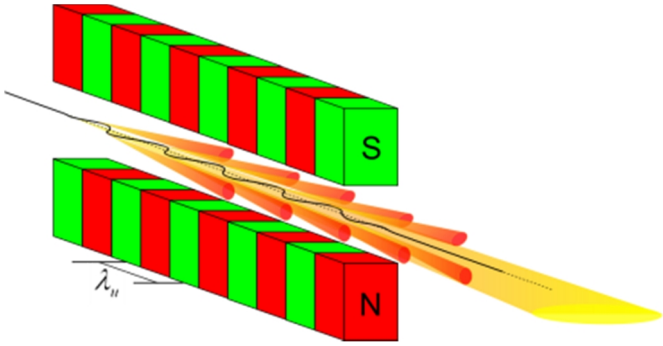

Figure 7. Operating principle of an undulator [22]. Electrons enter the magnetic structure which causes the electrons to oscillate in plane perpendicular to the direction of propagation. As a result, the emitted radiation will exhibit interference.

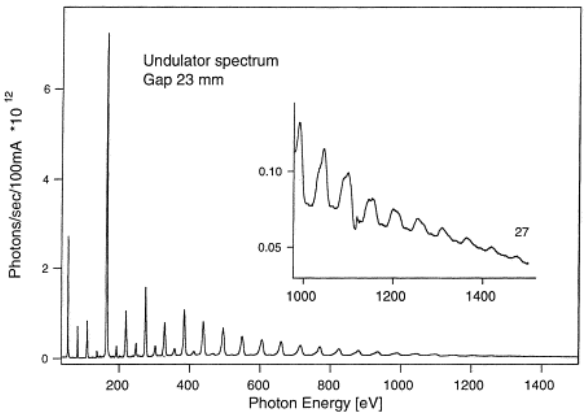

Figure 8. Undulator spectra of beamline I411 of the MAX-lab synchrotron radiation facility [23].

The energy of the emitted photons can be controlled by changing the magnetic field of the undulator. In practice, the adjustable parameter is the gap between the magnets. The polarization of the radiation can also be selected by changing the relative positions of the magnetic structure arrays. An additional problem arises from the higher harmonics of the undulator radiation which are result of a non-constant velocity of the electron in the direction of its propagation. Higher harmonics can be useful if higher photon energies are needed, but more often their presence is not required. With

VUV radiation, these higher harmonics can be blocked by a filter, e.g. LiF window, placed before the experimental chamber.

3.1.3 Beamlines

In this thesis work, all the experiments using synchrotron radiation were performed in the former MAX-lab synchrotron radiation facility in Lund, Sweden. There was no booster ring in the MAX-lab, but the electrons were injected from the linear accelerator directly to the storages rings presented in Figure 9.

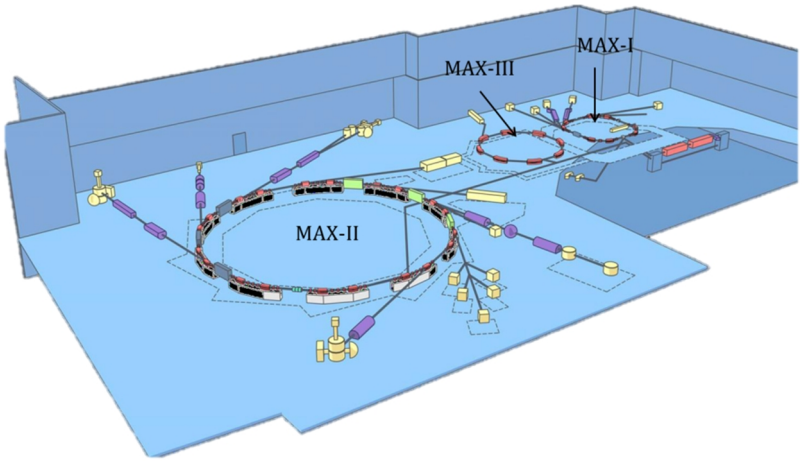

Figure 9. Storage rings of the former MAX-lab in Lund, Sweden. Picture is taken from ref. 24 with modifications.

Measurements with VUV radiation were carried out at beamline I3 [25] which was located at the MAX III storage ring that had a circumference of 36 m and an operating energy of 700 MeV. The photon energy range of beamline I3 was 5-50 eV with a resolving power E/dE of the order of 10^5. The radiation was monochromatized using a normal incidence monochromator (NIM) with changeable gratings. In all of the measurements included in this thesis work, a MgF_2/Al coated grating with 2400 lines/mm was used.

Measurements using soft x-rays were performed at beamline I411 [26] of the MAX II storage ring that had a circumference of 90 m and an operating energy of 1.5 GeV. The photon energy range of beamline I411 was 40-1500 eV with a resolving power $E/dE \sim 10^3$–10^4. The radiation was mono-

chromatized with a modified Zeiss SX-700 plane-grating monochromator with 1220 lines/mm.

3.2 Spectroscopic techniques

3.2.1 Time-of-flight mass spectroscopy

In ion time-of-flight mass spectroscopy (ion TOF MS), ions with different mass-to-charge ratios *m/q* are separated in time. This is achieved by giving an equal amount of energy to ions with the same charge *q*, causing velocities of the ions to depend on their *m/q* ratios. Thus, heavier ions move more slowly and the time required for the ions to reach the detector can be converted into an *m/q* scale. The relationship between the flight time *T* and the mass-to-charge ratio of an ion can be expressed as an equation

$$T = T_0 + C\sqrt{\frac{m}{q}}\ , \tag{10}$$

where T_0 and C are calibration constants that depend on the spectrometer and measurement settings.

In practice, the ions with same charge are given a fixed amount of energy by accelerating them in an electric field. After acceleration, suitable time delays between ions of different masses are induced by leading them into a field-free region or a drift space before their detection. The first spectrometer of this type emerged already in 1948 [27], but a sufficient mass resolution for scientific investigations was only achieved during the 1950's. The famous article by Wiley and McLaren in 1955 [28] proposed a two-stage acceleration process which improved the mass resolution significantly. In the first stage, a voltage V_s is applied over the sample region in order to direct all the ions towards the acceleration region (see Figure 10). The voltage V_s is called the extraction voltage and thus the sample region is sometimes referred to as the extraction region. In the second acceleration stage, the ions are accelerated with a voltage of V_d after which they will enter the drift space or the drift tube.

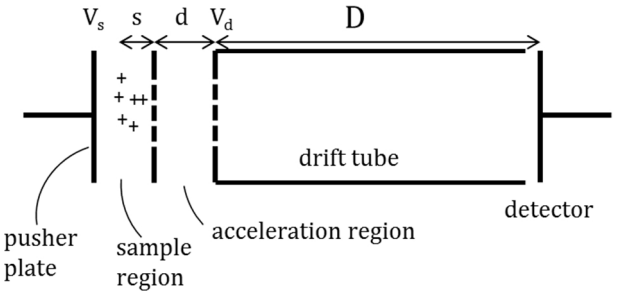

Figure 10. The main parts of a Wiley–McLaren type time-of-flight spectrometer.

The purpose of the two-stage acceleration is to compensate for the spatial distribution of the ions. The ions formed closer to the pusher plate will acquire slightly more energy and will have higher velocities than the ions that formed closer to the acceleration region. Thus the ions of the same *m/q* ratios formed in different positions in the sample region will have different flight times resulting in wide peaks in the spectrum. By selecting appropriate voltages V_d and V_s (and corresponding electric fields E_d and E_s), it is possible to focus the flight times of ions of the same *m/q*. It can be shown [29] that the position D_0 where the faster ions will eventually overtake the slower ions of the same *m/q*, is given by equation

$$D_0 = 2s_0 k_0^{3/2}\left(1 - \frac{1}{k_0 + k_0^{1/2}}\frac{d}{s_0}\right) \tag{11}$$

where *d* is the length of the acceleration region as shown in Figure 10, s_0 is the position where the ion is formed and $k_0 = 1 + (d/s_0)\cdot(E_d/E_s)$. Therefore, by changing the ratio E_d/E_s it is possible to focus the ion flight times and adjust the resolution of the mass spectra. The combination of applied voltages V_s and V_d that enable the fast and slow ions of the same *m/q* ratios to arrive at the detector at the same time is called *the Wiley–McLaren space-focusing condition*.

The starting time for the measurement of the flight times may be determined by using a pulsed ionization source or by using pulsed extraction voltages V_s. The major advantage of the latter is that it can be used in coincidence spectroscopy where the electron detection signal triggers the extraction pulse and determines the starting time of the flight time measurements (see Section 3.2.3).

3.2.2 Electron spectroscopy

Emitted electrons from ionized samples carry with them information about the electronic structure of the molecules. According to the Koopmans' approximation, ionization energy is equal to the negative value of the orbital energy (Eq. 8). Therefore, the best experimental approximation of the molecular orbital energies can be obtained by analyzing the photoelectron spectra. Auger electrons, on the other hand, can be used to study the final state populations in multiply ionized molecules (see Section 2.4). In both cases, the analysis starts by measuring the kinetic energies of the electrons. In this thesis work, all electron spectra were measured using a hemispherical analyzer.

A hemispherical analyzer consists of two concentric hemispherical electrodes that are held at different potentials. Electrons emitted from the sample are collected and guided between the hemispheres by lens systems placed in front of analyzer's entrance slit. The average radius of the spheres, nominal radius r_0, determines the dispersion and the resolution of the analyzer. The induced electric field between the electrodes is such that only electrons with a certain energy E_0 will follow a path with r_0 radius. Deviations from this nominal energy E_0 cause the electrons to have a slightly different path and to arrive at different positions at the detector. Moreover, since the electric field is spherically symmetrical, the analyzer focuses the electrons with the same energy but which enter the analyzer at different angles to the same x-coordinate of the detector (see Figure 11). This improves the transmission by increasing the acceptance angle of the electrons.

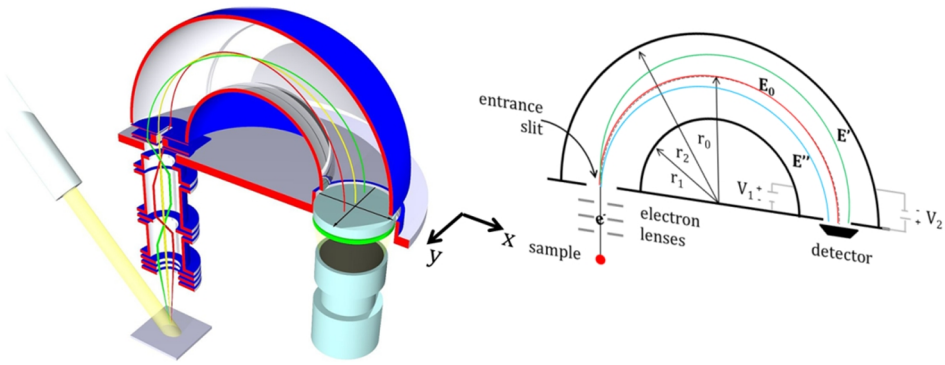

Figure 11. Operating principle of a hemispherical analyzer. (The left image is taken from ref. 30.) The path of an electron inside the analyzer depends on its energy. The electrons with the same energies are spatially focused on the same x-coordinate.

The base resolution of a hemispherical analyzer is given by

$$\frac{\Delta E}{E} = \frac{s_1 + s_2}{2r_0}, \tag{12}$$

where s_1 and s_2 denote the entrance and exit slit widths, respectively, and r_0 is the nominal radius as shown in Figure 11. If a position sensitive analyzer is used, the exit slit width can be replaced by the accuracy of the detector or ignored altogether, which improves the resolution significantly. In addition to providing better resolution, using position sensitive analyzers improves the measured intensity since electrons can be detected from larger area.

The hemispherical analyzer can be operated with a constant relative resolution (Eq. 12) or with a constant absolute resolution ΔE_a. In photoelectron measurements, the latter mode is usually more practical. However, at high kinetic energies good absolute resolution is difficult to achieve. This problem can be overcome by retarding the electrons before they enter the analyzer. The actual energy of the electrons after the retardation is called pass energy. With constant pass energy E_{pass}, the absolute resolution in becomes

$$\Delta E_a = E_{pass} \frac{s_1}{2r_0}, \tag{13}$$

providing that the width of the exit slit can be ignored as, for example, when using position sensitive detectors. The entrance slit width and the pass energy can usually be both adjusted to select a combination of resolution and transmission that accommodate the demands of the experiment.

3.2.3 Coincidence spectroscopy in photofragmentation studies

Combining the information from mass and electron spectroscopic measurements provides more profound understanding about ionization and subsequent fragmentation processes than using either of the spectroscopies exclusively. Different coincidence techniques, where multiple particles originating from the same ionization event are detected simultaneously, have proven to be especially valuable in investigations of various radiation-related phenomena. In this thesis work, photoelectron-photoion-photoion coincidence or PEPIPICO spectroscopy was employed to study the fragmentation of core-ionized biomolecules. In PEPIPICO, ions are analyzed with TOF MS using the detection signal of the emitted photoelectron as the starting point for the flight time measurements. This type of coincidence technique was first introduced by Frasinski *et al*. [31] and Eland *et al.* [32] in

1986. Four years later, Hanson *et al.* introduced another type of electron-ion-ion coincidence technique where ions are detected in coincidence with the emitted Auger electrons [33]. This technique was originally named ERAEMICO (energy-resolved, Auger electron, multiple-ion coincidence) mass spectroscopy. In this thesis work, however, abbreviation AEPIPICO is used.

Results of PEPIPICO or AEPIPICO measurements are often presented as two-dimensional maps where the flight time of the heavier ion is plotted versus the flight time of the lighter ion. An example of these *photoion-photoion coincidence* or *PIPICO maps* is provided in Figure 12.

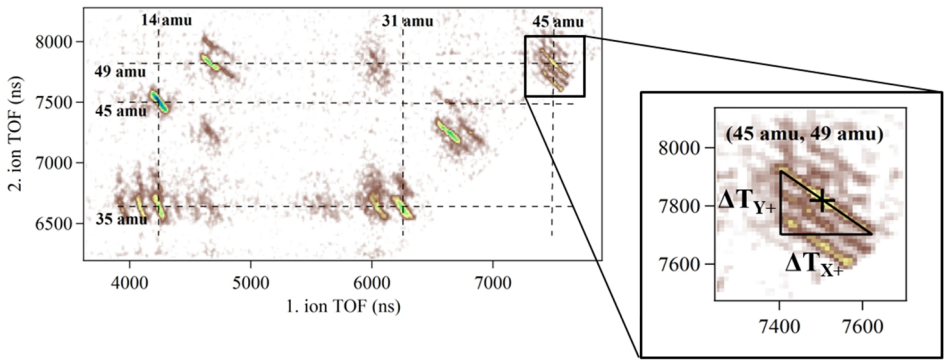

Figure 12. PIPICO map of chloroacetic acid measured in coincidence with Cl LVV Auger electrons. The enlargement indicates the flight time deviations used in determination of the slope and the pattern length. The cross-hairs mark the masses of the ion pairs at flight times corresponding to no initial kinetic energy of ions.

The tilted line-like patterns in PIPICO maps originate from fragmentation processes where kinetic momenta of the fragment ions remain correlated after fragmentation. The correlation is also manifested in velocities of the ions and results in deviation in their observed flight times (see the enlargement in Figure 12). As explained in ref. 34, the slopes of such patterns,

$$k = \frac{\Delta T_{Y^+}}{\Delta T_{X^+}}, \tag{14}$$

contain information about the fragmentation sequence, whereas the lengths of the patterns,

$$l = \sqrt{\Delta T_{X^+}{}^2 + \Delta T_{Y^+}{}^2}\ , \tag{15}$$

can be used to calculate how much kinetic energy is released in the dissociation process. Patterns with irregular shapes, on the other hand, originate

from concerted fragmentation processes in which the molecule breaks into multiple fragments in an explosion-like manner, losing the correlation of the kinetic momenta of the fragments completely or to a large extent.

One of the most challenging aspects of the electron-ion coincidence technique is minimizing the effect of false coincidences. When more than one sample molecule $\mathcal{M}$ is ionized at the same time, there is a possibility that the electron and ion detected simultaneously do not originate from the same ionization event (see Figure 13). These so-called false coincidences contribute to background noise in coincidence data. One way to attend to this problem is to decrease the ionization rate, i.e. to reduce the number of events occurring simultaneously. The obvious disadvantage of this method is increased data collection time. Another option, usually applied in combination with low counting rates, is to use artificial triggers to collect a dataset with false coincidence events which can then be used to statistically reduce the effect of the false coincidences from the coincidence data [35]. However, this method is only approximate and does not remove the effect of false coincidences entirely.

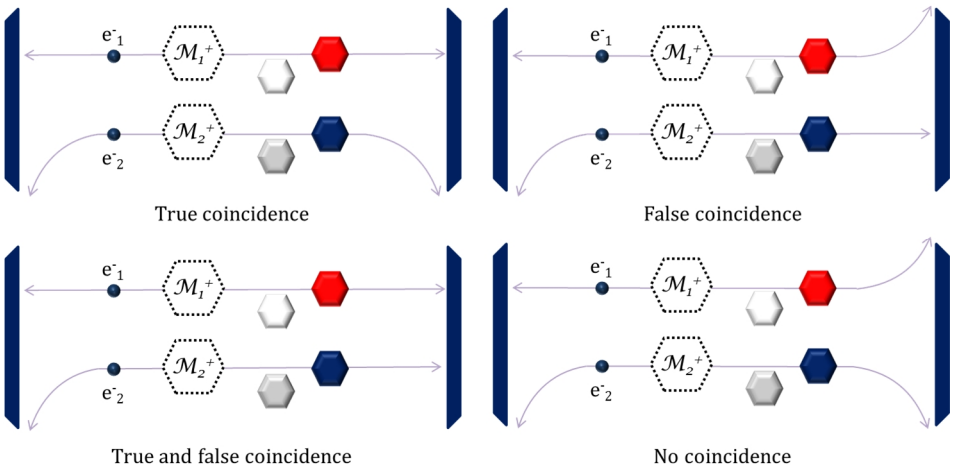

Figure 13. Schematic of true and false coincidence events.

3.3 Equipment and techniques

3.3.1 The spectrometers

Molecular cations created by ionization were detected with a home-made Wiley-McLaren type ion time-of-flight (ion TOF) spectrometer with a Ha-

mamatsu 77 mm active area multichannel plate (MCP) detector. The spectrometer was used in pulsed mode in which the extraction pulse starts the time counter for the flight times of the ions.

Kinetic energies of the electrons were analyzed by hemispherical electron analyzers. Part of the measurements belonging to paper IV was performed with a modified Omicron EA-125 analyzer in which the original channeltron detector was replaced by a 40 mm active area diameter resistive anode detector (RAD), made by Quantar. The original HV power and the detector power supplies were replaced by home-made units and the control system and software were also replaced. In all other measurements (papers III, V, VI and partly IV), the analyzer was a modified Scienta SES-100 where again the original CCD camera was replaced by a resistive anode detector.

In coincidence measurements, the ion mass spectrometer was combined with the electron analyzer in a similar manner as shown in Figure 14. This coincidence spectrometer setup was developed by Kukk *et al.* and the detailed description of its operating system can be found in ref. 36. The influence of false coincidences was reduced by using low counting rates of less than 25 electrons/s and by using artificial triggers provided by a pulse generator (see Section 3.2.3).

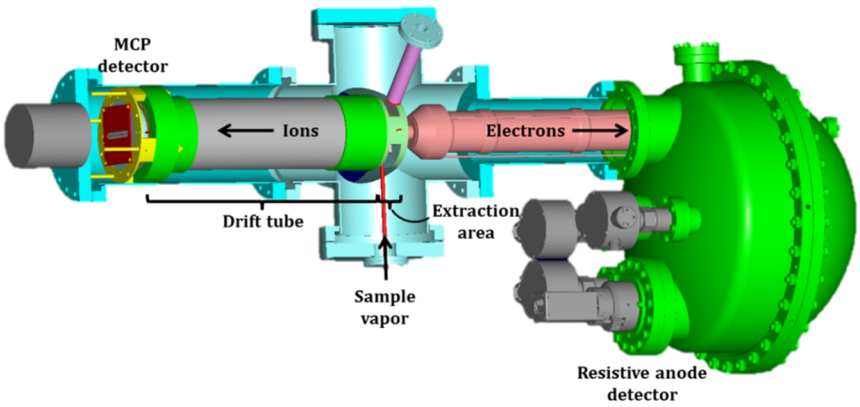

Figure 14. Schematic view of an ion-electron coincidence spectrometer setup similar to the spectrometer used in this thesis work.

3.3.2 Sample preparation

All the samples studied in this thesis work were purchased from Sigma-Aldrich and were used without further purification. If necessary, solid samples were introduced into gas phase by vaporizing them from a crucible of

resistively heated oven (MBE Komponenten NTEZ40). The vaporizing temperature was measured with a thermocouple, incorporated in the bottom of the crucible. Most of the studied biomolecules were easily deteriorated by the heat and the vaporizing temperature had to be kept relatively low, typically below 160 °C. In addition, possible thermal degradation of the molecule was monitored during the experiments by comparing TOF spectra measured during heating. In case of coincidence experiments that could take nearly an hour per measurement, TOF spectra were recorded regularly between separate coincidence measurements. During the measurements, pressure inside the spectrometer was between 10^{-7}–10^{-5} mbar.

3.3.3 Data analysis

All measured data, either simple mass spectra or more complicated PEPIPICO data, were analyzed using Igor Pro software with custom data analysis tool kit macros. The main parameter to be analyzed from the mass spectra was the intensities of the peaks which were obtained by spectral fitting with the least-squares method using SPANCF macro tool kit [37-38]. The data from PEPIPICO measurements was analyzed using another set of customized macros [35], and the analysis was mainly based on the PIPICO maps. With the help of these maps, different ion pair regions can be defined, and the ion pair intensities (counts per electron trigger) within a region can be extracted. These ion intensities can also be plotted against the kinetic energies of the coincident electrons resulting in *photoion-photoion yield* or *PIPIY curves*. Another important feature to be analyzed from PIPICO maps was the shapes of the ion pair patterns. As explained in Section 3.2.3, the shapes of the patterns contain information about the fragmentation sequence and the energy released in the process.

The derivation of the PIPICO pattern slopes (Eq. 14) in various fragmentation scenarios is well documented in ref. 40. Therefore, only results for the fragmentation processes relevant to this thesis work are repeated here for the convenience of the reader. The most important fragmentation pathways encountered in this thesis work are *two-body dissociation*, *deferred charge separation*, *secondary dissociation*, and *symmetrical charge separation followed by secondary dissociations*.

In two-body dissociation, a molecular dication consisting of A, B, C and D moieties dissociates exactly into two fragment ions:

$$ABCD^{++} \rightarrow \begin{cases} AB^{+} \\ CD^{+} \end{cases}.$$

This dissociation process results in patterns with slopes $k = -1$.

In deferred charge separation, a neutral fragment is detached before charge separation:

$$ABCD^{++} \rightarrow \begin{cases} AB \\ CD^{++} \end{cases} \rightarrow \begin{cases} AB \\ C^{+} \\ D^{+} \end{cases}.$$

In this case, the slope of the pattern is approximately –1, assuming that the kinetic energy release in the first phase is negligible.

In secondary dissociation, the charge separation occurs before the detachment of a neutral fragment:

$$ABCD^{++} \rightarrow \begin{cases} A^{+} \\ BCD^{+} \end{cases} \rightarrow \begin{cases} A^{+} \\ B^{+} \\ CD \end{cases}.$$

The slope of the pattern now depends on whether the heavier ion is separated in the first or in the second phase. If the cation A^{+} is heavier than the cation B^{+}, the slope is determined by equation:

$$k = \frac{\Delta T_{A^{+}}}{\Delta T_{B^{+}}} \approx -\frac{m_{BCD^{+}}}{m_{B^{+}}} \tag{16}$$

where $m_{BC^{+}}$ and $m_{B^{+}}$ are the masses of the *BC* and *B* moieties of the molecule, respectively. If the cation B^{+} is heavier than the cation A^{+}, the slope is reciprocal value of Eq. 16.

The last fragmentation sequence to be considered here is the symmetrical charge separation followed by secondary dissociations:

$$ABCD^{++} \rightarrow \begin{cases} AB^{+} \\ CD^{+} \end{cases} \rightarrow \begin{cases} A^{+} \\ B \\ C^{+} \\ D \end{cases}.$$

In this case, the slope is determined by

$$k = \frac{\Delta T_{A^+}}{\Delta T_{C^+}} \approx -\frac{m_{A^+}}{m_{C^+}} \cdot \frac{m_{CD^+}}{m_{AB^+}} \tag{17}$$

assuming that the cation A^+ is heavier than the cation C^+. In the opposite case, the slope is again determined by reciprocal value of Eq. 17.

4 RESULTS AND CONCLUSIONS

4.1 Functional group effects in nucleosides – papers I-III

The VUV radiation induced fragmentation of the DNA nucleoside thymidine ($C_{10}H_{14}N_2O_5$) and the RNA nucleoside uridine ($C_9H_{12}N_2O_6$) was studied with ion TOF MS. These molecules were introduced into gas phase by heating. In order to exclude the possibility of thermal deterioration, a suitable working temperature was first established by measuring mass spectra at different temperatures and observing the changes in the spectra. A chemistry book published in the 1970's already instructed that thermal deterioration of nucleosides occurs as a rupture of the glycosidic bond, accompanied by hydrogen transfer from sugar to base [40]. By examining the ratio of the base cation B^+ and the cation $(B+H)^+$ that can only come from undeteriorated sample over different temperatures, one can thus establish the onset of thermal degradation.

In paper I, we investigated thermal deterioration of thymidine in detail by examining the behavior of all detected fragments as a function of temperature and concluded that thermal deterioration indeed occurs as dissociation between the sugar and the base part. In addition, our analysis verified that examining the ratio of different base cations, $(B+H)^+/B^+$ is a viable means to study thermal degradation and, therefore, it was used to find a suitable measurement temperature in the continuation study on the fragmentation of nucleosides (paper II). We found that the RNA nucleoside uridine is less fragile against thermal effects, the onset of deterioration being between the measurements taken at 140 and 145 °C, whereas in the

DNA nucleoside thymidine it was found to be between 138 and 140 °C. In paper II, we also investigated a third nucleoside, 5-methyluridine ($C_{10}H_{14}N_2O_6$), which was observed to be even more resilient against thermal deterioration. It was not observed to exhibit any deterioration in the temperature range up to 170 °C.

Based on the thermal deterioration studies mentioned above, the highest temperature at which no deterioration was observed was chosen in order to maximize the sample vapor pressure, and that temperature was used as a measurement point in photofragmentation analysis. We found that VUV radiation induced fragmentation of all the studied nucleosides, thymidine, uridine and 5-methyluridine, was dominated by glycosidic bond rupture and possible hydrogen transfer. Because 5-methyluridine differs from uridine and thymidine only by one methyl and one hydroxyl group (see Figure 15), comparing their fragmentation behavior gives insight into the effect of functional groups on the photofragmentation of nucleosides. We arrived at the following conclusions: i) the extent and the site of fragmentation are affected more by the hydroxyl group in the sugar part than by the methyl group in the base, ii) adding a hydroxyl group makes the sugar moiety more fragile and facilitates charge migration from sugar to base, and iii) hydroxyl group and methyl group together have a combined effect in stabilizing the nucleoside against thermal deterioration.

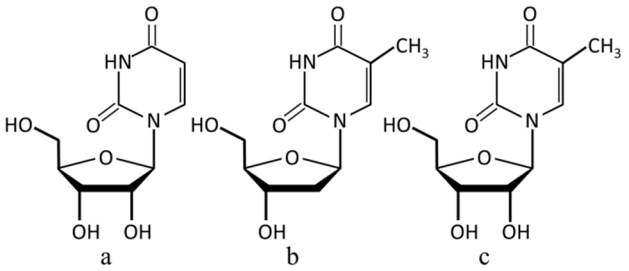

Figure 15. Structures of uridine (a), thymidine (b), and 5-methyluridine (c).

The fragmentation of core-ionized thymidine [41] and core-ionized uridine (paper III) has also been studied by our group and the results are in good agreement with the findings of valence ionization studies. Although core ionization leads to extensive fragmentation of both nucleosides, the fragment pairs of core-ionized uridine also contain combination fragments, i.e. fragments where the glycosidic bond is intact. Combination fragments were also observed to be relatively abundant in valence-ionized uridine. On

the contrary, combination fragments were absent in core-ionized and were very weak in valence-ionized thymidine. The difference in the amounts of combination fragments between thymidine and uridine was explained by the more fragile D-ribose ring compared with deoxy-D-ribose ring leading to bond breakage across the D-ribose ring rather than across the glycosidic bond.

4.2 The effects of substitutes in acetic acid – paper IV

Carboxylic acids contain a carboxyl group attached to a hydrocarbon chain of varying length or a cyclic hydrocarbon molecule. The simplest amino acid, glycine, can be made from a carboxylic acid called acetic acid by substituting only one hydrogen atom with an amine group. Replacing another hydrogen atom with a methyl group would lead to formation of another amino acid, alanine, and with further substitutions, plenty of other amino acids could be made. Studying the properties of acetic acid, therefore, provides a good starting point in amino acid studies. Moreover, being a relatively simple molecule, acetic acid is a good test sample to investigate the effect of halogen substitutes in biomolecules.

The ionization-site dependent fragmentation of chloro- and bromoacetic acids (see Figure 16) was investigated in paper IV. The fragmentation following the ionization of C 1*s* and Cl 2*p* or Br 3*d* core orbitals was studied by PEPIPICO measurements. In order to investigate the internal energy of the final dicationic state, the C KVV and Cl LVV or Br MVV Auger spectra were theoretically modeled. The outcome of the theoretical modeling was then verified by performing C KVV and Cl LVV Auger spectra measurements of chloroacetic acid. AEPIPICO measurements of chloroacetic acid following Cl 2*p* ionization were also performed in order to observe how internal energy possibly affects fragmentation pathways.

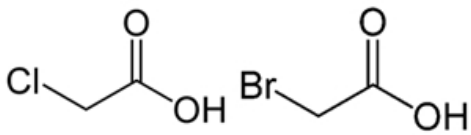

Figure 16. Chloroacetic acid ($ClC_2H_3O_2$) and bromoacetic acid ($BrC_2H_3O_2$).

PEPIPICO measurements revealed that both samples shared many similar fragmentation pathways. The branching ratios of different fragmentation pathways were observed to depend strongly on the ionization site. The

theoretical and experimental Auger spectra indicated that there is a clear difference in internal energies of the final dicationic state after ionizing carbon and halogen core orbitals in a way that the average internal energy is larger after C 1*s* core-hole decay. AEPIPICO measurements of chloroacetic acid confirmed that it is indeed the internal energy difference that causes the site-dependent behavior: fragmentation products resulting from fragmentation channels of higher final state energy were more abundant after C 1*s* ionization than after Cl 2*p* ionization, and vice versa.

Almost all fragmentation pathways of chloro- and bromoacetic acids were affected by the initial ionization site the same way. Thus, it appears that replacing the halogen substitute chlorine with bromine changes the extent, not the nature of the effect the halogen has on the molecule. It can also be concluded that the site-dependent fragmentation observed for chloro- and bromoacetic acids is of statistical nature altering only the relative abundances of different fragments, not the fragmentation pathways themselves. In other words, with a fixed final state energy, the fragmentation is identical, regardless of the ionization site.

4.3 Fragmentation of core-ionized amino acid L-α-alanine – unpublished data

In addition to the published papers on amino acids ([42-43], paper V), our research group has also studied fragmentation of core-ionized amino acid L-α-alanine ($C_3H_7NO_2$), hereafter referred to as alanine (see Figure 17). A part of the preliminary results of these investigations was used as complimentary material in a theoretical study on alanine [44], but the main results are published in this thesis for the first time.

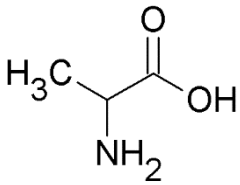

Figure 17. Structure of L-α-alanine.

4.3.1 AEPIPICO and PEPIPICO experiments

Fragmentation of core-ionized alanine was studied by PEPIPICO and AEPIPICO measurements with the coincidence measurement setup de-

scribed in Section 3.3.1. The electron analyzers in PEPIPICO and AEPIPICO measurements were Omicron EA-125 and Scienta SES-100, respectively. Detailed information on the measurement settings are provided in Table I.

Both PEPIPICO and AEPIPICO experiments were performed at beamline I411 of the former MAX-II synchrotron radiation facility (see Section 3.1.3). The sample with stated purity of ≥99.5 % was purchased from Sigma-Aldrich and was used without further purification. It was introduced to gas phase by heating, keeping the temperature below 132 °C.

Table I. Experimental details of coincidence measurements of alanine.

Measurement/ Ionization site	Photon energy (eV)	E_{pass} (eV)	Kinetic energy range (eV)	Entrance slit width (mm)	Energy resolution (eV)
PEPIPICO/C 1*s*	315	100	15-25	6	2.4
PEPIPICO/N 1*s*	425	50	16-22	6	1.4
AEPIPICO/N 1*s*	425	200	358-378	3.2	1.7

4.3.2 Results from PEPIPICO measurements

The measured PEPIPICO maps are presented in Figure 18. Both of the maps have similar ion pair patterns indicating same fragmentation pathways regardless of the ionization site. Six main ion pair regions can be distinguished from them (all masses are stated in atomic mass units): (14-15, 28), (14-15, 45), (17-18, 45), (27-28, 45), (29, 40-42), and (39-42, 45). The ion pairs (39-42, 45) are likely to be formed when the doubly charged alanine molecule dissociates into a singly charged carboxyl ion (45 amu) and a singly charged $CH_3CH(NH_2)^+$ moiety ion (44 amu) which further loses two or more hydrogens. This primary dissociation could then be followed by further fragmentation of the charged $CH_3CH(NH_2)^+$ moiety into a methyl group (15 amu), a $CH(NH)^+$ (28 amu) or CHN^+ (27 amu) moiety and neutral hydrogen(s). Depending on whether it is the methyl group or the CHN/CH(NH) moiety that retains the charge, ion pairs at masses (15, 45) and (27-28, 45) are observed. In the middle of these two regions, there are somewhat weaker patterns with masses (17-18, 45). The only possible assignments for these are pairs where the larger fragment corresponds to the carboxyl group and the smaller fragment corresponds to NH_3^+ or NH_4^+ ions.

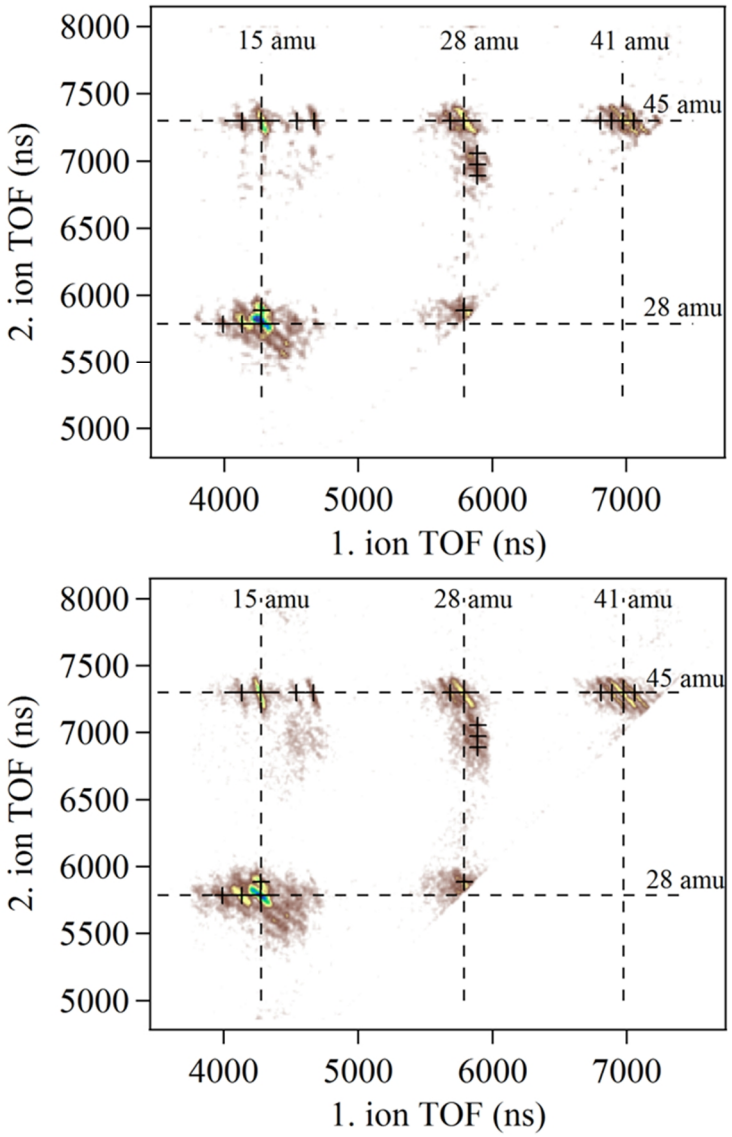

Figure 18. PIPICO maps of the amino acid alanine from N 1*s* ionization (top) and C 1*s* ionization (bottom). The cross-hairs mark the masses of the ion pairs at flight times corresponding to no initial kinetic energy of ions.

The ion pairs discussed above originate from a primary dissociation process where the carboxyl group detaches as an ion. It is also possible that the carboxyl group detaches as a neutral fragment and the charge remains in the $CH_3CH(NH_2)$ moiety. When this doubly charged ion fragments further, the pairs (14-15, 28) are observed. These ions likely correspond to CH_2N^+

(28 amu) and CH_2^+ (14 amu) or CH_3^+ (15 amu) ions, with one or two neutral hydrogen(s) released in the fragmentation process.

A simple carboxyl group detachment and possible secondary dissociation cannot explain the ion pairs (29, 40-42). Based on their masses, the pair (29, 42) could correspond to fragments (COH^+, CNO^+), ($C_2H_5^+$, CNO^+) or (COH^+, $C_2NH_4^+$). The first two assignments require a considerable amount of bond breakages and molecular rearrangements and they are regarded as unlikely cases. The last pair assignment, however, could be explained by neutral water molecule loss from alanine with sequential two-body dissociation into ions COH^+ and $C_2NH_4^+$. Further hydrogen loss would explain the other pairs in this region.

For the dissociation pathways described above, the slopes of the ion-ion patterns should be -1 for the ion pairs (39-42, 45), (29, 40-42), (13-15, 28) and (15, 29), -3 for (14-15, 45), -2.6 for (17, 45), -2.4 for (18, 45), and -1.6 for (27-28, 45). All of these values agree reasonably well with the slope estimations of the observed patterns presented in Figure 19.

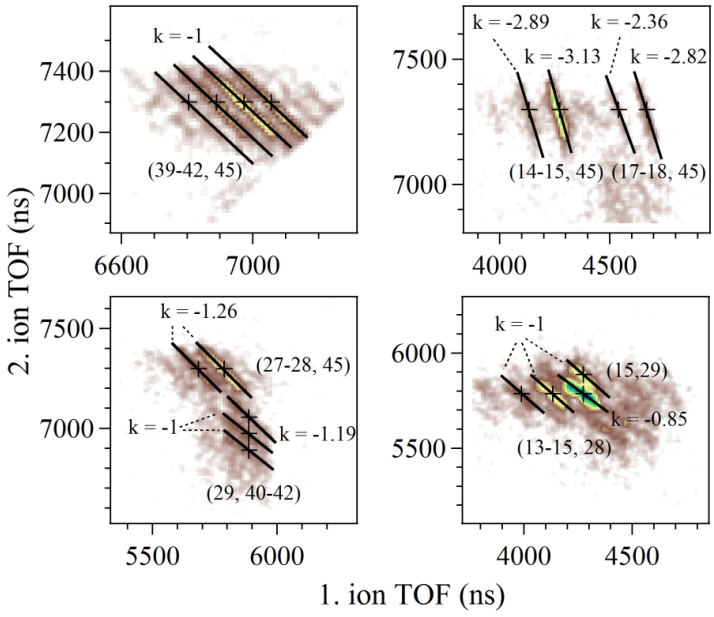

Figure 19. Estimated slopes for the ion pair patterns in the C 1*s* PIPICO map (Figure 18). The cross-hairs mark the masses of the ion pairs at flight times corresponding to no initial kinetic energy of ions.

The internal energy dependence of the fragmentation of alanine was studied with AEPIPICO measurements after ionization of the N 1*s* core orbital. Ion pair yields of the stronger fragment pairs of alanine were extracted from the AEPIPICO data with similar methods as described in paper IV and the result is shown in Figure 20. With exceptions of the pairs (14, 28) and (18, 45), all ion pairs behave similarly having a maximum at the kinetic energy of approximately 372 eV. Behavior of the pair (14, 28) is different from the other pairs, but the high background makes further interpretations impossible. The high background in this ion pair signal comes from ionization of the residual gas nitrogen. Since the alanine sample is prone to thermal degradation, its molecular density had to remain rather low and the signal from N_2 was in fact the dominant one. While it directly affects only the (14, 14) ion pairs, it also generates a very strong false coincidence background with sample ions coupled to either N^+ (14 amu) or N_2^+ (28 amu, from valence ionization of N_2) ions. The ion pair yield curve of (18, 45), however, resembles the other curves but has its maximum at higher kinetic energy values. It can be concluded that most of the fragment pairs of alanine result from dicationic final states corresponding to similar energies. Interestingly, the pair (18, 45) is produced in higher kinetic energy or lower internal energy channels, requiring on average even less energy to form than the two-body dissociation. One possible explanation for this can be found in molecular dynamics [45]. Formation of an NH_4^+ ion requires migration of two hydrogens from other parts of the molecule to the amine group. When hydrogens attach to the amine group, the bond between NH_2 and the carbon atom is immediately broken. Such a process does not require more energy than a two-body dissociation; however, it is a very slow process and leads to low intensities of the ions.

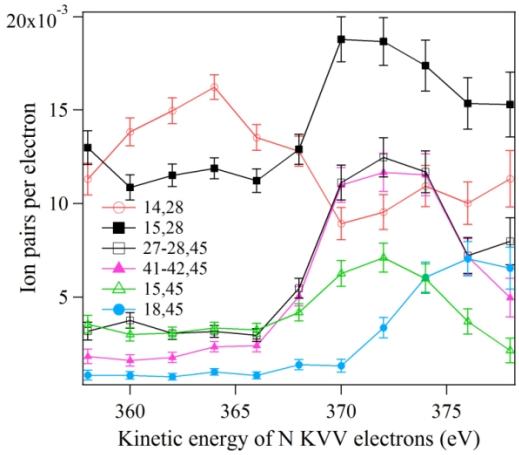

Figure 20. Ion pair yields of the fragments of alanine as a function of the kinetic energy of Auger electrons. The error bars indicate statistical uncertainties.

4.3.3 Conclusions

All observed fragmentation pathways of the core-ionized alanine conform to either of the following dissociation sequences: i) separation of a neutral or charged carboxyl group, followed by a possible secondary dissociation of the $CH_3CH(NH_2)$ moiety or ii) loss of a neutral water molecule followed by two-body dissociation of the remaining part of the molecule. Fragmentation pathways were observed to be the same in C 1*s* and N 1*s* ionization. Most of the fragment pairs were also observed to have similar dependence on the internal energy of the dicationic final state of alanine.

4.4 Structural effects in amino acids – papers V and VI

Amino acids comprise a carboxyl group -COOH and an amine group -NH_2. These functional groups can be attached to the same carbon atom (alpha amino acids) or to adjacent carbons (beta amino acids). Moreover, the majority of amino acids has two stereoisomers, L-form and D-form, which are mirror images of each other. Almost all biologically relevant amino acids, however, exist in L-α-form [46], leaving differences between different amino acids in the length and composition of their side chains. Therefore, examining different L-α-amino acids not only provides biologically relevant information on their photofragmentation but also gives insight into the influence of side chains on the physical properties of the amino acids. All amino acids studied in this thesis work were of L-α- form, and in the following, the prefix L-α- is not repeated.

4.4.1 Fragmentation pathways and the degree of fragmentation

This thesis work contains studies on three core-ionized amino acids: alanine (Section 4.3), cysteine (paper V) and serine (paper VI). These amino acids differ from each other only by one atom; replacing one hydrogen atom in alanine's CH_3 side chain with an SH-group or OH-group produces cysteine and serine molecules, respectively (see Figure 21). The fragmentation of cysteine was studied after site-selective ionization of four core orbitals: C 1*s*, O *1s*, S 2*p*, and N 1*s*. The fragmentation of serine and alanine, however, was only studied after ionization of two sites: O 1*s* and C 1*s* (serine), and N 1*s* and C 1*s* (alanine). Since all of them were studied with C 1*s* ionization, this ionization site is taken as a point of comparison to reveal differences in their fragmentation behavior.

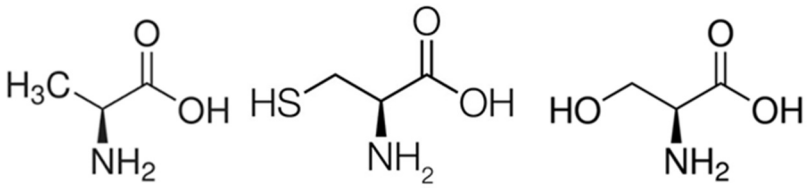

Figure 21. L-α-amino acids alanine ($C_3H_7NO_2$), cysteine ($C_3H_7NO_2S$), and serine ($C_3H_7NO_3$).

The main dissociation pathways of cysteine were observed to be the following: i) separation of a neutral or charged carboxyl group followed by a possible secondary dissociation, ii) sequential dissociation starting with separation of the charged SH-group, and iii) concerted fragmentation. The fragmentation pathway i) was also observed in serine and alanine. Two other main dissociation pathways of serine were found to include separation of a neutral side chain followed by secondary dissociation, and sequential dissociation after separation of a charged OH-group (from carboxyl group). Alanine, on the other hand, was observed to have only one other fragmentation pathway in addition to the process i): the loss of a neutral water molecule followed by secondary dissociation. The main dissociation pathways were concluded to yield in eight different fragment products in cysteine when ions differing only by the number of hydrogens were considered as one group. The same numbers for serine and alanine were four and six, respectively. Thus, cysteine appears to fragment in a more versatile way than alanine or serine.

In addition to the fragmentation pathways, it is interesting to consider the degree of fragmentation in each amino acid. The versatility of fragmentation pathways in itself is not a very good indicator of fragility of molecules because it does not say anything about how big a proportion of the molecules remains intact upon ionization. Our measurements did not reveal doubly charged parent molecules of amino acids; the least destructive form of fragmentation observed was the dissociation into two ions, which requires rupture in only one bond. Therefore, two criteria are used here to assess the degree of fragmentation in amino acids: 1) how big a proportion of product ions result from two-body dissociation and 2) how big a proportion of product ions requires breakages in multiple bonds. For the sake of simplicity, bonds between hydrogens and other atoms are not considered. Based on these criteria, alanine appears to be the most resilient amino acid against radiation: two-body dissociation covers 20 % of product ions of alanine, whereas two-body dissociation is virtually non-existent in serine and in cysteine. Moreover, all other fragments pairs of alanine result from rupture in only two bonds. Two-bond breakage in serine and cysteine, in contrast, amounts for nearly 97 % and 90 % of ions, respectively. Ions requiring breakage of at least three bonds constitute ca. 3 % of fragments of serine and ca. 10 % of fragments of cysteine. The conclusion is that despite having only a few ways to fragment, radiation damage to serine is more extensive than to alanine, and the most fragile of all the three amino acids is cysteine.

4.4.2 Effects of ionization site

Fragmentation of alanine was also studied after ionizing N 1*s* core orbital, but no site-dependent effects were observed compared with C 1*s* ionization (see Section 4.3.2). Ionizing O 1*s* core orbital of serine did not result in different fragmentation behavior either, when compared with C 1*s* ionization. Cysteine, however, was observed to exhibit strong site-dependent effects between initial ionization sites of C 1*s*, S 2*p*, N 1*s* and O 1*s*. The smallest degree of fragmentation was observed in S 2*p* ionization. Compared with C 1*s* ionization, for example, the amount of two-body dissociation products in S 2*p* ionization increased approximately from 0 to 5 %, and the proportion of ions resulting from breakage of at least three bonds decreased approximately from 12 to 4 %. The reason for these site-dependent effects was concluded to be the difference in internal energy of the dicationic parent molecule (see Figure 2 in paper VI). Interestingly, differences in fragmenta-

tion behavior between different *sample molecules* could not be ascribed to the effects of internal energy. The average internal energy after the C 1*s* core hole decay in serine appeared to be similar to the average internal energy after the C 1*s* core hole decay in cysteine.

4.4.3 Comparison with glycine and methionine

The amino acid glycine ($C_2H_5NO_2$) provides an interesting point of comparison for amino acids studied in this thesis since its side chain only contains a hydrogen atom (see Figure 22). The previous study on core-ionized glycine [43] indicated that glycine has plenty of different ways to fragment; surprisingly more than the next simplest amino acid alanine. The most intense fragmentation pathways observed included loss of a carboxyl group followed by a possible secondary dissociation, and proton ejection. Proton ejection is probably a common process in all amino acids; unfortunately, the proton signal has been outside of measurement windows in other amino acid studies and confirmation of this is not possible. Two-body dissociation between the carboxyl group and the CH_2NH_2 moiety was also observed to be a very common process in glycine. It was observed to yield in approximately 28 % of ion pairs not originating from proton ejection [47]. This shows glycine as an even more robust molecule against soft x-rays than alanine.

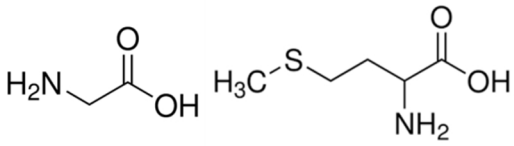

Figure 22. Structures of amino acids glycine (left) and methionine (right).

The final point of comparison is taken to be the amino acid methionine ($C_5H_{11}NO_2S$) that has a significantly longer side chain than the other amino acids discussed above (see Figure 22). The study on core-ionized methionine [42] concluded that all of its fragmentation pathways can be summarized as a separation of a carboxyl group followed by secondary dissociation in the remaining $CH(NH_2)CH_2CH_2SCH_3$ moiety. Thus, methionine does not exhibit two-body dissociation at all; moreover, the majority of its photofragments requires breakages of at least three bonds. This presents methionine as even more fragile against soft x-rays than cysteine.

4.4.4 Conclusions

Amino acids studied in this thesis work, cysteine, alanine and serine, were observed to have very different ways of fragmentation after core ionization. The only pathway common to all three was observed to be the loss of a carboxyl group followed by a possible secondary dissociation, which has been reported before as a common fragmentation process in amino acids [42-43, 48-51]. Comparing the minimum number of bonds required to break in order to form the observed fragment ions, it was concluded that fragility against soft x-rays increases in the order alanine < serine < cysteine. Since internal energy was observed to be similar in both serine and cysteine, the more extensive fragmentation of cysteine can only be a result of a more fragile molecular structure. Moreover, since neither alanine nor serine exhibits site-dependent fragmentation, adding a sulfur atom in the side chain appears to alter the molecular orbital structure in a more dramatic way than adding an oxygen atom.

Comparison with earlier studies on glycine and methionine placed them at the opposite ends on the fragility scale of amino acids: glycine being the least fragile and methionine being the most fragile of all amino acids considered here. Thus, it appears that mass (and possibly length) of the side chain determines the extent to which an amino acid fragments. However, further studies on amino acids with side chains of varying lengths *and* masses would be needed to verify this observation.

4.5 Conclusions

Comparison between three nucleosides revealed that adding or removing a single functional group can affect both the charge localization in fragments as well as the bonds that break to form the observed fragments. The latter effect can be so strong that it can be observed even with thirty times more energetic radiation. In addition to the effects on photofragmentation, the combined effect of two functional groups can have a surprising influence on the volatility of the molecule.

Studies on core-ionized halogenated acetic acids and amino acids indicated that one simple substitution can dramatically change the extent of fragmentation. Within a sample, the different fragmentation behavior following different ionization sites was ascribed to alterations in dicationic final state populations. However, comparison between different samples introduced another important factor contributing to fragmentation: the

composition of the molecule. Even with similar internal energies, the fragmentation behavior is not necessarily the same but depends on the molecular composition. Interestingly, both bromoacetic acid and cysteine contained heavier substitute elements than their points of comparison, chloroacetic acid and serine, and they were also observed to fragment more extensively than their counterparts. Thus, in order to control the extent of the fragmentation, it is not always necessary to alter the amount of energy inflicted on the molecule but selecting a proper substitute may suffice.

This thesis work demonstrates that the effects of structure and composition on the photofragmentation of biomolecules can efficiently be studied by coincidence spectroscopic methods and sometimes even with mass spectroscopic measurements alone. However, further studies with time-resolved measurements would be most interesting, especially in investigations of site-dependent effects. Following the charge location by pump-probe experiments with free electron lasers, for example, would be very beneficial in order to elaborate on the role of charge localization in the site-dependent effects. Observing the intermediate state of a dissociating molecule would also provide more information on the fate of the neutral fragments not seen by traditional spectroscopic methods.

References

[1] J. E. Penner-Hahn, *X-ray Absorption Spectroscopy*, Comprehensive Coordination Chemistry II. Elsevier 2003, 159.

[2] G. N. Dolenko, O. K. Poleshchuk, and J. N. Latośińska, *X-ray Emission Spectroscopy*, *Methods*, Encyclopedia of Spectroscopy and Spectrometry. Elsevier 1999, 2463.

[3] D. Zagorevskii, *Mass Spectrometry*, Comprehensive Coordination Chemistry II. Elsevier 2003, 367.

[4] D.-S. Yang, *Photoelectron spectroscopy*, Comprehensive Coordination Chemistry II. Elsevier 2003, 187.

[5] T. Arion and U. Hergenhahn, *Coincidence spectroscopy: Past, present and perspectives*, Journal of Electron Spectroscopy and Related Phenomena 200 (2015), 222.

[6] A. van der Kogel and M. Joiner (ed.), *Basic Clinical Radiobiology*, 4th edition. Hodder Arnold 2009, 11.

[7] H. N. Chapman, C. Caleman, and N. Timneanu, *Diffraction before destruction*, Philosophical Transactions of The Royal Society B 369 (2014), 20130313.

[8] D. R. Hartree, *The Wave Mechanics of an Atom with a Non-Coulomb Central Field. Part I. Theory and Methods*, Mathematical Proceedings of Cambridge Philosophical Society 24 (1928), 89.

[9] J. C. Slater, *The self consistent field and the structure of atoms*, Physical Review 32 (1928), 339.

[10] J. C. Slater, *Note on Hartree's method*, Physical Review 35 (1930), 210.

[11] V. Fock, *Näherungsmethode zur Lösung des quantenmechanischen Mehrkörperproblems*, Zeitschrift für Physik 61 (1930), 126.

[12] P. W. Atkins and R. Friedman, *Molecular quantum mechanics,* 5th edition. Oxford University Press 2011, 262, 298, 304.

[13] S. F. Boys, *Electronic Wave Functions. I. A General Method of Calculation for the Stationary States of Any Molecular System*, Proceedings of the Royal Society A 200 (1950), 542.

[14] R. Ditchfield, W. J. Hehre, and J. A. Pople, *Self-Consistent Molecular-Orbital Methods. IX. An Extended Gaussian-Type Basis for Molecular-Orbital Studies of Organic Molecules*, The Journal of Chemical Physics 54 (1971), 724.

[15] M. M. Francl, W. J. Pietro, W. J. Hehre, J. S. Binkley, M. S. Gordon, D. J. DeFrees, and J. A. Pople, *Self-consistent molecular orbital methods. XXIII. A polarization-type basis set for second-row elements*, The Journal of Chemical Physics 77 (1982), 3654.

[16] W. J. Hehre, R. Ditchfield, and J. A. Pople, *Self-Consistent Molecular Orbital Methods. XII. Further Extensions of Gaussian—Type Basis Sets for Use in Molecular Orbital Studies of Organic Molecules*, The Journal of Chemical Physics 56 (1972), 2257.

[17] P. C. Hariharan and J. A. Pople, *The influence of polarization functions on molecular orbital hydrogenation energies*, *Theoretica Chimica Acta* 28 (1973), 213.

[18] M. W. Schmidt, K. K. Baldridge, J. A. Boatz, S. T. Elbert, M. S. Gordon, J. H. Jensen, S. Koseki, N. Matsunaga, K. A. Nguyen, S. Su, T. L. Windus, M. Dupuis, and J. A. Montgomery, *General atomic and molecular electronic structure system*, Journal of Computational Chemistry 14 (1993), 1347.

[19] http://www.webmo.net/ (referenced 4.2.2016)

[20] C. R. Brundle, and A. D. Baker (ed.), *Electron spectroscopy : theory, techniques and applications vol. 1*. Academic Press 1977, 186.

[21] http://www.chemicalghosts.org/research/synchrotron-science/ (referenced 16.11.2015).

[22] http://photon-science.desy.de/research/studentsteaching/primers/synchrotron_radiation/index_eng.html (referenced 16.11.2015).

[23] M. Bässler, A. Ausmees, M. Jurvansuu, R. Feifel, J.-O. Forsell, P. de Tarso Fonseca, A. Kivimäki, S. Sundin, S. L. Sorensen, R. Nyholm, O. Björneholm, S. Aksela, and S. Svensson, *Beam line I411 at MAX II—performance and first results*, Nuclear Instruments and Methods in Physics Research 469 (2001), 382.

[24] https://www.maxlab.lu.se/node/153 (referenced 16.11.2015).

[25] S. Urpelainen, M. Huttula, T. Balasubramanian, R. Sankari, P. Kovala, E. Kukk, E. Nõmmiste, S. Aksela, R. Nyholm, and H. Aksela, *FINEST: a high performance branch-line for VUV photon energy range gas phase studies at MAX-lab*, AIP Conference Proceedings 1234 (2010), 411.

[26] M. Bässler, J.-O. Forsell, O. Björneholm, R. Feifel, M. Jurvansuu, S. Aksela, S. Sundin, S. L. Sorensen, R. Nyholm, A. Ausmees, and S. Svensson, *Soft X-ray undulator beam line I411 at MAX-II for gases, liquids and solid samples*, Journal of Electron Spectroscopy and Related Phenomena 101 (1999), 953.

[27] B. A. Mamyrin, *Time-of-flight mass spectrometry (concepts, achievements, and prospects)*, *International Journal of Mass Spectrometry* 206 (2001), 251.

[28] W. C. Wiley and I. H. McLaren, *Time-of-Flight Mass Spectrometer with Improved Resolution*, Review of Scientific Instruments 26 (1955), 1150.

[29] N. Mirsaleh-Kohan, W. D. Robertson, and R. N. Compton, *Electron ionization time-of-flight mass spectrometry: historical review and current applications.*, Mass Spectrometry Reviews 27 (2008), 237.

[30] https://de.wikipedia.org/wiki/Photoelektronenspektroskopie (referenced 23.11.2015).

[31] L. J. Frasinski, M. Stankiewicz, K. J. Randall, P. A. Hatherly, and K. Codling, *Dissociative photoionisation of molecules probed by triple coincidence; double time-of-flight techniques*, Journal of Physics B 19 (1986), L819.

[32] J. H. D. Eland, F. S. Wort, and R. N. Royds, *A photoelectron-ion-ion triple coincidence technique for the study of double photoionization and its consequences*, Journal of Electron Spectroscopy and Related Phenomena 41 (1986), 297.

[33] D. M. Hanson, C. I. Ma, K. Lee, D. Lapiano-Smith, and D. Y. Kim, *Single-event, energy-resolved, Auger–electron, multiple-ion coincidence mass spectroscopy*, The Journal of Chemical Physics 93 (1990), 9200.

[34] E. Itälä, *Fragmentation processes in organic molecules induced by synchrotron radiation*, doctoral thesis, University of Turku 2013, 38-44.

[35] E. Kukk, *PEPICO data analysis – Software for Igor Pro – User's manual*, University of Turku 2014.

[36] E. Kukk, R. Sankari, M. Huttula, A. Sankari, H. Aksela, and S. Aksela, *New electron-ion coincidence setup: Fragmentation of acetonitrile following N 1s core excitation*, Journal of Electron Spectroscopy and Related Phenomena 155 (2007), 141.

[37] E. Kukk, G. Snell, J. D. Bozek, W.-T. Cheng, and N. Berrah, V*ibrational structure and partial rates of resonant Auger decay of the N 1 s → 2 π core excitations in nitric oxide*, Physical Review A 63 (2001), 062702.

[38] E. Kukk, K. Ueda, U. Hergenhahn, X.-J. Liu, G. Prümper, H. Yoshida, Y. Tamenori, C. Makochekanwa, T. Tanaka, M. Kitajima, and H. Tanaka, *Violation of the Franck-Condon principle due to recoil effects in high energy molecular core-level photoionization.*, Physical Review Letters 95 (2005), 133001.

[39] D. T. Ha, *Theoretical Modelling and Experimental Studies of Synchrotron Radiation Induced Molecular Dissociation Processes*, doctoral thesis, University of Turku 2013, 30-36.

[40] P. O. P. Ts'o (ed.), *Basic principles in nucleic acid chemistry*, *vol. 1*. Academic Press 1974, 256-257.

[41] E. Itälä, M. A. Huels, E. Rachlew, K. Kooser, T. Hägerth, and E. Kukk, *A comparative study of dissociation of thymidine molecules following valence or core photoionization*, Journal of Physics B 46 (2013), 215102.

[42] D. T. Ha, Y. Wang, M. Alcami, E. Itälä, K. Kooser, S. Urpeainen, M. A. Huels, E. Kukk, and F. Martín, *Fragmentation Dynamics of Doubly Charged Methionine Phase*, The Journal of Physical Chemistry A 118 (2014), 1374.

[43] E. Itälä, K. Kooser, E. Rachlew, M. A. Huels, and E. Kukk, *Soft x-ray ionization induced fragmentation of glycine*, The Journal of Chemical Physics 140 (2014), 234305.

[44] Y. Wang, H. Levola, E. Rossich, D. Piekarski, S. Díaz-Tendero, E. Kukk, M. Alcamí, and F. Martín, *X-ray induced fragmentation dynamics of doubly charged L-alanine in gas phase*, Journal of Physics Conference Series 635 (2015), 112094.

[45] Private communication with D. T. Ha.

[46] J. McMurry, *Fundamentals of organic chemistry,* 7th edition, Brooks/Cole 2011, 505, 508.

[47] Data courtesy of E. Itälä.

[48] R. R. T. Marinho, A. F. Lago, M. G. P. Homem, L. H. Coutinho, G. G. B. de Souza, and A. Naves de Brito, *Gas phase photoabsorption and mass spectra of l-alanine and l-proline in the soft X-ray region*, Chemical Physics 324 (2006), 420.

[49] O. Plekan, V. Feyer, R. Richter, M. Coreno, and K. C. Prince, *Valence photoionization and photofragmentation of aromatic amino acids*, Molecular Physics 106 (2008), 1143.

[50] H.-W. Jochims, M. Schwell, J.-L. Chotin, M. Clemino, F. Dulieu, H. Baumgärtel, and S. Leach, *Photoion mass spectrometry of five amino acids in the 6–22 eV photon energy range*, Chemical Physics 298 (2004), 279.

[51] M. Morita, M. Mori, T. Sunami, H. Yoshida, and A. Hiraya, *Ionic fragmentation processes of core-excited α-alanine in gas phase*, Chemical Physics Letters 417 (2006), 246.